

## Structure, soft modes, and superconductivity in Cl-doped cadmium sulfide

S. Bilodeau,\* D. Campbell,<sup>†</sup> R. K. MacCrone, and S. J. Nettel

*Department of Materials Engineering and Department of Physics, Rensselaer Polytechnic Institute, Troy, New York 12180-3590*

(Received 12 June 1987)

Previous measurements on pressure-quenched CdS have revealed anomalous magnetic susceptibility indicative of high-temperature superconductivity, but only over a narrow critical range of chlorine doping. X-ray-diffraction studies as a function of chlorine doping now show that at the critical chlorine doping the material undergoes a phase transition, leaving it as wurzite. Photoacoustic spectroscopy shows that a soft lattice mode appears just beyond critical doping, over the same range as the anomalous magnetism. Lastly, we find by analysis that superparacurrent is induced by a magnetic field in wurzite, providing the lattice mode associated with the wurzite zinc-blende phase transition is very soft.

### INTRODUCTION

Para- and diamagnetism of a magnitude suggesting superconductivity at around 200 K has been observed in pressure-quenched CdS. The CdS must be doped with a critical concentration of chlorine.<sup>1-4</sup> In this paper we report on progress in understanding these phenomena.

Experiments have been carried out on the unpressurized but doped CdS. We have largely succeeded in elucidating the complex structural transformations to which the material is subject. The correlation we have found between structural properties and the unusual magnetic properties provide a basis for a model and a theoretical calculation.

Doping by chlorine plays an important role in the occurrence of the high-temperature superconductivity. It has been found that there exists a critical concentration, hereafter designated  $C^*$ . It is well known that the doping of CdS with chlorine in unpressurized material induces a gradual transition from the zinc-blende to the wurzite structure, 100% wurzite being realized at about 3 wt. % chlorine.<sup>5,6</sup> Furthermore, it is also well known that chlorine stabilizes the cubic high-pressure phase, cubic sodium chloride structure, when the pressure is released to ambient.<sup>7</sup> Again, about 3 wt. % chlorine completely prevents the sodium chloride from reverting to wurzite zinc blende; a greater fraction of material reverts as the chlorine content is reduced, and 100% reversion occurs in undoped material. The sensitivity of the appearance of our magnetic states on chlorine content after pressure quenching suggests that other conventional physical properties will also be sensitive to chlorine content in the same range. Conversely, these physical property variations provide insights into the mechanism of the superconductivity.

For simplicity, and as a first step in a long-range study, here we have studied and characterized the unpressurized starting material. In particular, we have measured the photoacoustic effect (PA effect) as a function of chlorine content, and studied the structure of the wurzite by x-ray diffraction.

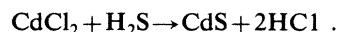
The x-ray results show that the relative amount of zinc-blende to wurzite phase is not as gradual a function

of chlorine content as has previously been assumed; rather the transformation occurs most rapidly at chlorine contents in the vicinity of  $C^*$ . The wurzite itself shows an abrupt change in the  $c$  lattice parameter (by  $\sim 0.5\%$ ) on crossing  $C^*$ , suggesting the existence of two different hexagonal phases. The PA results show that the zinc-blende-wurzite phase transformation is soft-mode driven, and most significantly, the soft modes abruptly disappear at chlorine contents above  $C^*$ . At the same time the x-ray line broadening shows that the stacking fault probability in the wurzite is increasing rapidly for chlorine content above  $C^*$ . The extensive stacking faulting in the wurzite phase above  $C^*$  is equivalent to having a wurzite-zinc-blende mixed structure. In consequence, we believe the soft modes in question are the transverse shear modes close to that mode  $q$  which takes the wurzite into the sodium chloride structure; namely modes with a  $k$  vector parallel to the [0001] direction with transverse polarization in the  $[10\bar{1}0]$  direction, the [111] and [112] directions, respectively, in the resultant zinc-blende structure. In the theory part, we show that the excitation of these modes in wurzite by the application of a magnetic field gives rise to supercurrents.

### EXPERIMENT

#### Experimental methods

The material was prepared by precipitation from aqueous solution according to the reaction



The amount of chlorine incorporated into the precipitates depends on the pH of the solution; the details have been described by Cote *et al.*<sup>8</sup> Following this procedure a series of samples with increasing chlorine content have been prepared, the actual chlorine content being determined using neutron-activation analysis and ion chromatography.<sup>9</sup> The x-ray structural studies were carried out on the powders using a conventional Philips diffractometer.

The photoacoustic spectroscopy was determined using a Princeton Applied Research photoacoustic cell and

preamplifier. The specimens consisted of disks of pressed powder 2.5 mm in diameter. The modulus of the acoustic signal was obtained by adding the squares of the in-phase and quadrature components.

## EXPERIMENTAL RESULTS

### X-ray diffraction

A series of diffractometer recordings are shown in Figs. 1(a)–1(d), each trace being from a specimen of different chlorine content. As can be seen, the intensities of the diffraction peaks from the zinc-blende cubic phase decrease at the expense of the wurzite lines with increasing chlorine content, indicating the well-known<sup>5,6</sup> stabilization of the wurzite. At the same time the wurzite lines broaden, this being associated with stacking faults in the structure. By convention, the fraction hexagonal stacking  $w_h$  is given by<sup>10</sup>

$$w_h = 4R / (3R + 1.33),$$

where  $R$  is given by

$$R = I_{10.0} / (I_{00.2} + I_{111}),$$

$I_{hk_0l}$  and  $I_{hk_1}$  being the intensity of the hexagonal and cu-

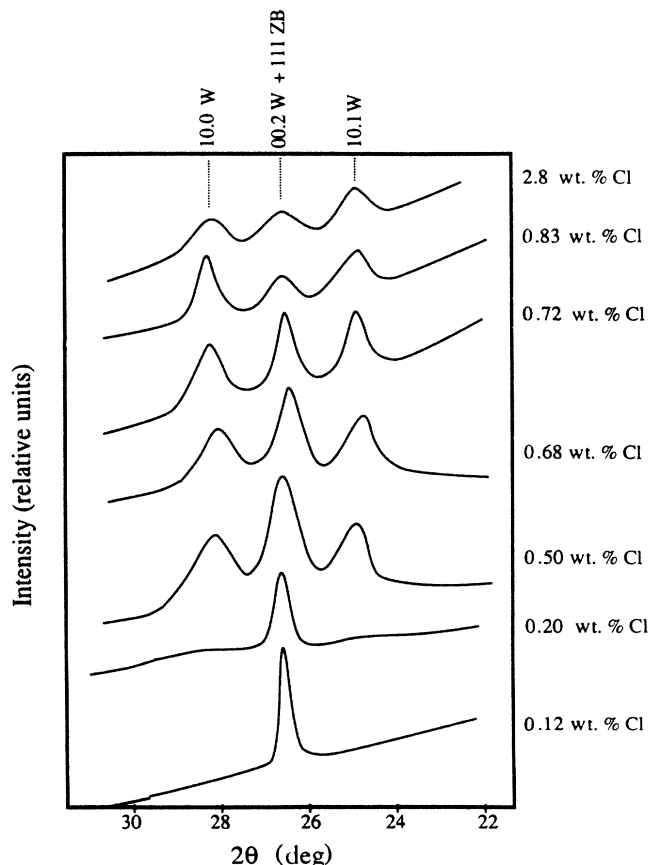


FIG. 1. X-ray-diffraction intensity over a range of  $2\theta$  where the cubic and hexagonal lines overlap. As the chlorine doping increases, the hexagonal phase ( $w$ ) increases at the expense of the cubic phase (ZB).

bic lines, respectively. The quantity  $w_h$  is shown plotted in Fig. 2, which shows that the amount of cubic phase present in the vicinity of  $C^*$  is strongly dependent on chlorine content. The chlorine content at which the greatest sensitivity occurs is just below  $C^* = 0.7$  wt. %.

The angular positions of the peaks associated with the hexagonal phase were determined by fitting the diffraction-peak maxima to a parabola using the method of Koistinen and Marburger<sup>11</sup> and the lattice parameters  $a$  and  $c$  determined as a function of chlorine content by a least-squares fit to the peak positions in each case. The results are shown in Fig. 3. As can be seen, the  $c$  parameter is nearly constant as the chlorine content is increased, followed by a precipitous drop in value at  $C^*$ . The  $a$  lattice parameter is insensitive to chlorine content. Last, we have also assessed the stacking-fault probability by quantitatively measuring the linewidths and analyzing the data following Warren<sup>12</sup> (note the increase in wurzite linewidths with increasing doping in Fig. 1). We find that the stacking-fault probability below 0.3 wt. % chlorine is essentially zero, followed by an increase to about 0.1 as we go through  $C^*$ .

The photoacoustic response is shown as a function of chlorine content in Fig. 4. As can be seen, the photoacoustic response increases gradually up to  $C^*$ , at which point the value drops precipitously to a lower value and remains constant for higher chlorine contents. Qualitatively, the important behavior is independent of the energy of the exciting light, suggesting that the response is of lattice origin rather than from effects of the chlorine on the band structure. Indeed, the relatively small step height of the PA signal when scanning the light energy across the band gap implies that we are in the so-called saturation regime.

Physically, saturation describes a condition where the photoacoustic signal is no longer proportional to the absorption coefficient  $k$ . In the saturation regime  $k$  is so large compared to the specimen thickness that all the light energy is absorbed within the specimen thickness. The PA response is then determined by the variations in the thermal properties rather than variations in the optical-absorptive properties. This assertion is so much

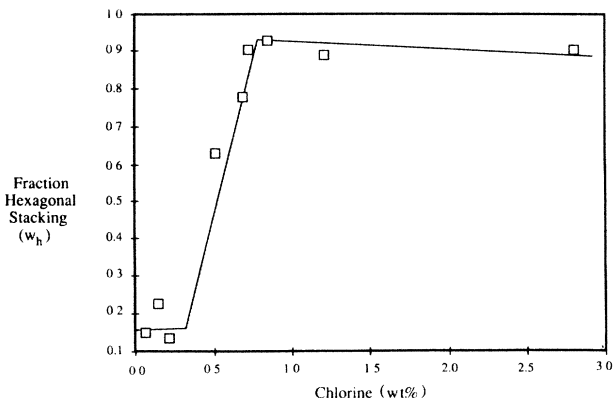


FIG. 2. Fraction hexagonal stacking  $w_h$  as a function of chlorine doping, deduced from x-ray-diffraction data as in Fig. 1. Note the rapid change in  $w_h$  in the vicinity of  $C^*$ .

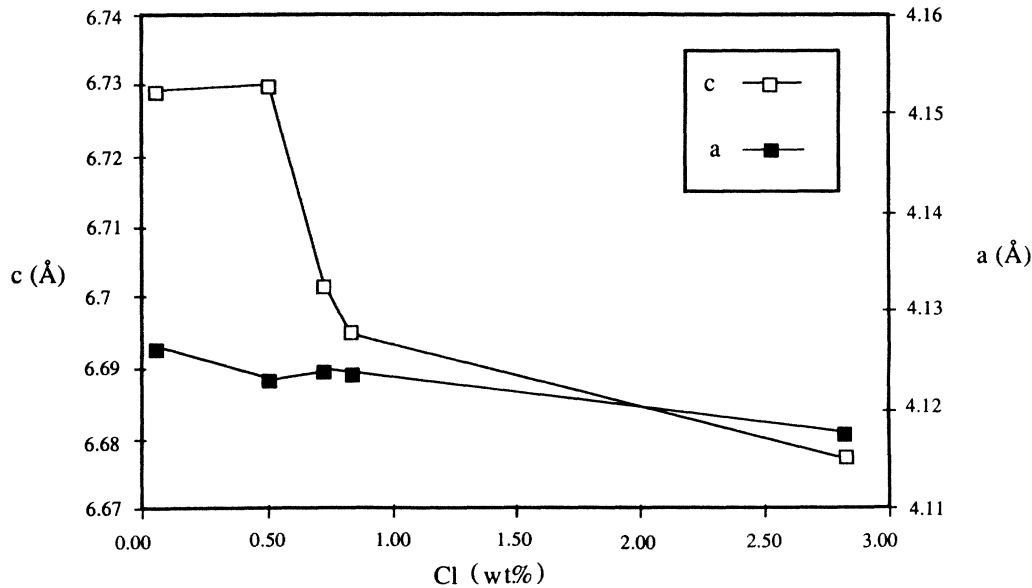


FIG. 3. Lattice parameters  $c$  and  $a$  of the wurzite only as a function of chlorine doping. Note the rapid change in  $c$  at  $C^*$ .

more true for the light of energy above the band gap (e.g., 2.4 eV) where the absorption is very large compared to the light of energy below the band gap (e.g., 2.0 eV).

In the saturation regime, the PA response is given by<sup>13</sup>

$$Q = (K\rho C_v)^{-1/2}.$$

Quantitatively, we find that a decrease by a factor of 25 in the value of  $k\rho C_v$  is required to account for our observations. Such large variations in  $C_v$  due to chlorine doping does not seem reasonable. For example, soft-mode contributions to the specific heat are, at reasonable concentrations, too small to account for the effect at room temperatures. We accordingly seek an explanation based on changes in the thermal conductivity. Impurity scattering

from the chlorine impurities is untenable, since the doping concentration varies smoothly across the range of interest. We may, therefore ascribe the rapid drop in the PA signal at  $C^*$  to a rapid change in the thermal conductivity brought about by the additional phonon-phonon scattering involving the soft modes. Florian *et al.*<sup>4</sup> have observed similar peaks in the PA spectrum to those in Fig. 4 during the cubic-to-orthorhombic phase transition in  $K_2SnCl_6$  as the sample was heated through 263 K. Raman spectroscopy<sup>15</sup> confirmed that the latter was a soft-mode-driven displacive phase transition accompanied by a reduction in the elastic constants.<sup>16</sup> Thermoacoustic and thermoelastic effects during phase transitions are discussed in general by Karpium, Tilgner, and Schmid<sup>17</sup> and by Junge, Bein, and Pelzl.<sup>18</sup>

Particle-size variations with chlorine content, as well as strain, cannot account for the PA results. Scanning-electron-microscopy observations of the powder samples used in Fig. 4 showed a constant spherical shape independent of chlorine doping. X-ray data showed little variation in size up to about 2 wt. % chlorine and then a slow decrease at the higher chlorine content. The strain in the particles, which was also measured by x-ray diffraction, showed a slight maximum at about 2 wt. % chlorine, but was constant at lower concentrations and, in particular, across compositions spanning  $C^*$ .

In summary in combining x-ray structural studies with photoacoustic spectroscopy we have found that the unpressurized CdS changes structure unexpectedly and abruptly at the critical chlorine content  $C^* = 0.7$  wt. %. Below  $C^*$  the structure is mainly cubic zinc blende with some wurzite. Above  $C^*$  it is mainly wurzite with a slightly smaller value of the lattice constant  $c$  than obtained below  $C^*$ . The wurzite above  $C^*$  is heavily stacking faulted, or, equivalently, wurzite mixed with zinc-blende structure. The soft modes, which are the ones that take wurzite into zinc-blende structure, are unequivocally confined to the region just around  $C^*$ . This is

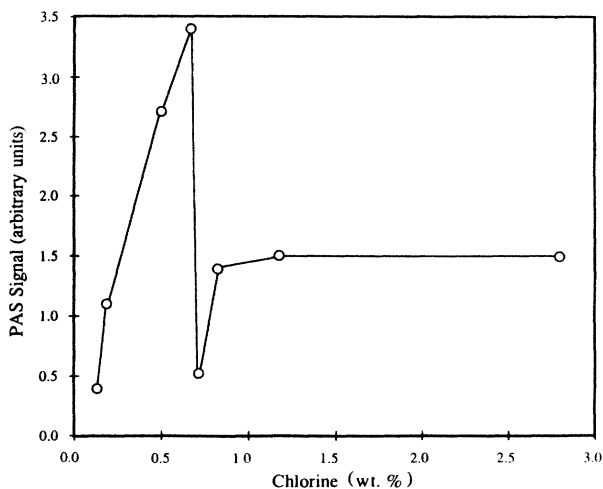


FIG. 4. Photoacoustic signal as a function of chlorine doping. These data were obtained using 2.0-eV light; between 2.0 and 2.4 eV, the behavior is identical, but the signal increases slightly with increasing energy. Note the discontinuity at  $C^*$ .

precisely the region where superconductivity has been observed. The soft modes linking these two structures play the critical role in the theoretical interpretation of superconductivity which now follows.

## THEORY

### Motivation

Our hypothesis for the origin of supercurrents in a marginally stable lattice follows from an analysis of an ordinary insulator. As a model for the insulator we choose a Hamiltonian

$$H_I = T + H_q + H_A + H_{AA} . \quad (1)$$

Here  $T$  is the kinetic-energy operator for a free-electron gas,  $H_q$  is the interaction of the electrons with the standing lattice modes of wave vector  $q$  above, and  $H_A$  and  $H_{AA}$  are the usual linear and quadratic interaction terms with an applied field  $\mathbf{A}$ .  $H_q$  creates the gap which separates the filled valence band from the empty conduction band. Otherwise the electrons are taken as free, i.e., a metallic situation prevails. We shall take  $\mathbf{A}(\mathbf{r})$  to be in the  $x$  direction. It will suffice to take only one standing-wave component,  $2\mathbf{A}(Q)\cos Qz$ , propagating in the  $z$  direction.

Following a paper on the Meissner effect by Wentzel<sup>19</sup> we eliminate at the outset the linear term in  $\mathbf{A}$  in the Hamiltonian with a unitary transformation, and subsequently solve the secular equations which yield Bloch waves. Physically the elimination of  $H_A$  may be regarded as a generalized Larmor transformation.

For the insulator, if  $\tilde{H}_I \equiv e^{-K_I} H_I e^{K_I}$  ( $K_I^* \equiv -K_I$ ) is the transformed Hamiltonian, one chooses

$$[T, K_A] = -H_A , \quad (2a)$$

$$[T, K_{qA}] = -H_{qA} \quad \text{where } H_{qA} = [H_q, K_A] , \quad (2b)$$

$$[T, K_{qqA}] = -H_{qqA} \quad \text{where } H_{qqA} = [H_q, K_{qA}] , \quad (2c)$$

$$K_I = K_A + K_{qA} + K_{qqA} + \dots , \quad (2d)$$

which yields

$$\tilde{H}_I = T + H_q + H_{AA} + \text{other higher-order terms in } A . \quad (3)$$

The electronic current operator is made up of the usual momentum current  $\mathbf{J}(Q)$ , along with  $-\mathbf{J}_A = -e^2 n \mathbf{A}/mV$ , where  $n/V$  is the density of electrons. The transformed current operator  $\tilde{\mathbf{J}}(Q)$  is given to first order in  $A$  by

$$\tilde{\mathbf{J}}(Q) = \mathbf{J}(Q) + [\mathbf{J}(Q), K_A] + [\mathbf{J}(Q), K_{qA}] + \dots . \quad (4)$$

In an insulator, in contrast to a superconductor, the expectation value of  $\tilde{\mathbf{J}}(Q)$  must be exactly canceled by  $-e^2 n \mathbf{A}/mV$  in the limit as  $Q \rightarrow 0$ . For the free-electron gas, Wentzel shows directly that this cancellation actually takes place.<sup>19</sup> Using a simple model of an insulator described below we have verified by direct calculation that the first few terms of the series in Eq. (4) are of the

correct order of magnitude in the limit  $Q \rightarrow 0$  to cancel the term  $-\mathbf{J}_A$ . This additionally substantiates our calculations using Wentzel's procedure, and shows dominance by the leading terms.

The observation that terms such as  $H_{qA}$  are giving rise to supercurrents in insulators, albeit compensated, suggests that the addition of similar new potentials to the Hamiltonian, i.e., terms with wave vectors  $\pm \mathbf{q} \pm \mathbf{Q}$ , will lead to further supercurrents, which, however, will be uncompensated. Such potentials can be generated by the electron-phonon interaction, piezoelectric for CdS, providing phonon modes are occupied macroscopically. The proposed scheme, reminiscent of a superconductor mechanism studied by Frohlich and others,<sup>19,20</sup> differs in that we are suggesting simultaneous excitation of many different modes, rather than just one. The soft-mode  $q$  which represents displacements leading from the cubic to the hcp lattice structure is assumed present, and for every standing-wave component  $\mathbf{A}(Q)$  of the applied magnetic field, components  $\pm \mathbf{q} \pm \mathbf{Q}$  are also present, but with smaller amplitudes.

The Frohlich mechanism has been criticized on the basis that the perturbation calculation on which it relies breaks down (no longer converges) at precisely the strength in the electron-phonon coupling where the superconductivity is first to be expected.<sup>21,22</sup> In our approach, perturbation theory plays a different role. The gap is created by the macroscopic excitation of the mode. As already indicated this mode introduces one of the Fourier components of the potential characterizing the wurzite phase. Its existence will be assumed as part of the unperturbed Hamiltonian, as we shall see. (The calculations of relative stabilities of different crystal structures from component ions and electrons are very difficult and need not be viewed as an explicit aspect of a supercurrent analysis.) The parts of our Hamiltonian which are treated as a perturbation come from the other modes,  $\pm \mathbf{q} \pm \mathbf{Q}$ . The interaction of the electron with these modes turns out to be proportional to the applied vector potential  $\mathbf{A}$ , and, in our linear analysis, is arbitrarily small.

We are suggesting that, in the material under consideration, the lattice is marginally stable, the mode  $q$  arising spontaneously. Excitation of additional modes such as  $\pm \mathbf{q} \pm \mathbf{Q}$ ,  $Q \rightarrow 0$  will, therefore, likewise entail only marginal expenditures of free energy. We shall carry through a semiquantitative variational calculation, which will show that the amplitudes of the modes  $\pm \mathbf{q} \pm \mathbf{Q}$  are proportional to the applied field  $\mathbf{A}(Q)$ . This latter field may, therefore, be thought of as applying a magnetic pressure on the lattice. Collecting all energy terms, we shall find that the usual electrodynamic term  $-\int \mathbf{A}_{-Q}(\mathbf{r}) \cdot \mathbf{J}_Q(\mathbf{r}) dv$ , with  $\mathbf{J}_Q(\mathbf{r})$  the  $Q$  component of the induced momentum current, is to be balanced against the marginal increase in lattice energy arising from the excitation of modes  $\pm \mathbf{q} - \mathbf{Q}$ .

For the insulator in a field the wave function will contain asymmetry. It can be found by applying the inverse unitary operator  $e^{K_I}$  to the lowest eigenstate of Eq. (3), resulting in a complicated combination of insulator eigenstates. The energy spectrum can be obtained in the (Larmor-) transformed system, and will be that of an or-

dinary insulator. [To second order in  $A$ , we treat  $H_{AA} + \dots$  in Eq. (3) as numbers rather than operators]. In the insulator  $H_A, H_{qA}, \dots$  induce electron distributions are unsymmetric in  $\mathbf{k}$  space, the center of symmetry being shifted to  $e\mathbf{A}/h$ , but the currents are compensated. Here the additional induced lattice potentials enhance the asymmetry. As a result of the additional asymmetry we shall find that there is net current while, as we shall see from the new Hamiltonian, the energy gap remains.

### Supercurrents

We, accordingly, generalize the unitary transformation of Eqs. (2), replacing  $K_I$  by  $K_I + K_S$ , where

$$[T, K_{qs}] \equiv -H_{qs}, \quad (5a)$$

$$[T, K_{qqs}] \equiv -H_{qqs} \quad (5b)$$

where

$$H_{qqs} \equiv [H_q, K_{qs}], \quad (5c)$$

$$K_S = K_{qs} + K_{qqs} + K_{qqqs} + \dots \quad (5d)$$

Here  $H_{qs}$  is the extra potential, and is linear in  $\mathbf{A}$ . The new Hamiltonian ( $H = H_I + H_{qs}$ ), transformed, becomes, to second order in  $\mathbf{A}$ ,

$$\bar{H} = T + H_q + H_{AA} + \frac{1}{2}[H_A + H_{qs}, K_I + K_S]. \quad (6)$$

The terms  $K_{qqs}, K_{qqqs}, \dots$  are found to have vanishing denominators as  $Q \rightarrow 0$ , and as Wentzel has pointed out<sup>19</sup> such terms give rise to significant momentum currents.

Explicitly,  $\mathbf{A}(Q)e^{-iQz}$  gives rise to a potential

$$H_{qs} = \sum_{kz < 0} \Lambda^*(k_x) a_k^* a_{k+q-Q} + \sum_{kz > 0} \Lambda(k_x) a_k^* a_{k-q-Q}. \quad (7)$$

Here the  $a^*, a$ , are free-electron creation and destruction operators.  $\Lambda^*, \Lambda$ , which are to be determined variationally, depend on the electron-phonon coupling constant and on the square root of the number of phonons in the

mode  $\pm\mathbf{q}-\mathbf{Q}$ .<sup>24</sup> In a real lattice (unlike in jellium) these coupling coefficients depend on  $\mathbf{k}$ , the location in reciprocal space where the electron scattering occurs. We are only concerned with their dependence on  $k_x$ . In the free-electron representation we consider only the states with  $-3q/2 < k_z < 3q/2$ , thereby limiting orbitals to combinations of states in the "vicinity of the gap," but obviously within generous limits.

$K_{qs}(-Q)$  defined by Eq. (5a) will be given by

$$K_{qs}(-Q) = \sum_{kz < 0} \frac{\Lambda^*(k_x) a_k^* a_{k+q-Q}}{E(k+q-Q) - E(k)} + \sum_{kz > 0} \frac{\Lambda(k_x) a_k^* a_{k-q-Q}}{E(k-q-Q) - E(k)} \quad (8a)$$

$$\equiv \sum_{kz < 0} K_{k, k+q-Q} a_k^* a_{k+q-Q} + \sum_{kz > 0} K_{k, k-q-Q} a_k^* a_{k-q-Q}, \quad (8b)$$

where the  $K_{k, k\pm q-Q}$  in Eq. (8b) are introduced for convenience.

The current density is given by

$$J(Q) = \frac{e\hbar}{2mcV} \sum_k (2\mathbf{k} + \mathbf{Q}) a_k^* a_{k+Q}. \quad (9)$$

The current  $\langle [J(Q), K_{qs}(-Q)] \rangle$  is odd in  $\mathbf{q}$ , and gives no net current, since we have both positive and negative  $q$ . The leading term in the induced supercurrent will be given by  $\langle [J(Q), K_{qqs}(-Q)] \rangle$ . We, accordingly, proceed to Eqs. (5b) and (5c).

We have, first,

$$H_q = \sum_{kz < 0} \Delta^*(k_x) a_k^* a_{k+q} + \sum_{kz > 0} \Delta(k_x) a_k^* a_{k-q}, \quad (10)$$

where the  $\Delta$ 's determine the crystal potential of the deformation  $q$ . From Eqs. (5c), (8), and (10), we again find with the restriction of  $k_z - 3q/2 < k_z < 3q/2$ , that

$$H_{qqs}(-Q) = \sum_{kz > 0} \Delta^*(k_x) K_{k, k-q-Q} (a_{k-q-Q}^* a_{k-q-Q} - a_k^* a_{k-Q}) + \sum_{kz < 0} \Delta(k_x) K_{k, k+q-Q} (a_{k+q-Q}^* a_{k+q-Q} - a_k^* a_{k-Q}) \quad (11)$$

and  $K_{qqs}(-Q)$  follows immediately from Eq. (5b). Equations (9) and (11) yield

$$[J(Q), K_{qqs}(-Q)] = \frac{e\hbar}{2mcV} \left[ \sum_{kz > 0} \Delta^*(k_x) K_{k, k-q-Q} [\mathbf{L}(\mathbf{k}, -\mathbf{q}-\mathbf{Q}) (a_{k-q-Q}^* a_{k-q-Q} - a_{k-q-Q}^* a_{k-q-Q}) - \mathbf{L}(\mathbf{k}, \mathbf{q}, \mathbf{Q}) (a_k^* a_k - a_{k-Q}^* a_{k-Q})] + \sum_{kz < 0} \Delta(k_x) K_{k, k+q-Q} (q \rightarrow -q) \right], \quad (12a)$$

where

$$\mathbf{L}(\mathbf{k}, \mathbf{q}, -\mathbf{Q}) \equiv (2\mathbf{k} + 2\mathbf{q} - \mathbf{Q}) / (E_{k+q} - E_{k+q-Q}). \quad (12b)$$

We now wish to take expectation values with respect to the ground state of  $T + H_q$ . To obtain Eq. (7) we have represented the orbitals in the eigenstates in a nearly-free-electron approximation as  $x_k^* a_k^* + y_k a_{k \pm q}^*$  for the lower band and  $y_k^* a_k^* - x_k a_{k \mp q}^*$  for the upper band. In evaluating Eq. (7) we shall adhere to this representation in the vicinity of the band edges where we find the current originates. The  $E(k)$  are one-electron energies in a band assumed parabolic. Taking into account that the lower band is filled, and the upper empty in the ground state, we find, with

$$X^2(\mathbf{k}, \mathbf{q}, -\mathbf{Q}) \equiv |x_{k+q}|^2 - |x_{k+q-Q}|^2, \quad (13a)$$

$$Y^2(\mathbf{k}, \mathbf{q}, -\mathbf{Q}) \equiv |y_{k+q}|^2 - |y_{k+q-Q}|^2, \quad (13b)$$

that

$$\langle [J(Q), K_{qs}(-Q)] \rangle = \sum_{i=1}^8 \hat{J}_i, \quad (14a)$$

$$J_1 = \frac{e\hbar}{2mV} \sum_{k_z > q/2} \Delta^*(k_n) K_{k, k-q-Q}^{-Q} [\mathbf{L}(\mathbf{k}-\mathbf{q}, -\mathbf{Q}) X^2(\mathbf{k}, -\mathbf{q}, -\mathbf{Q}) - \mathbf{L}(\mathbf{k}, 0, -\mathbf{Q}) Y^2(\mathbf{k}, -\mathbf{q}, -\mathbf{Q})], \quad (14b)$$

$$J_2 = \frac{e\hbar}{2mV} \sum_{k_z < -q/2} \Delta(k_n) K_{k, k+q-Q}^{-Q} [\mathbf{L}(\mathbf{k}+\mathbf{q}, -\mathbf{Q}) X^2(\mathbf{k}, \mathbf{q}, -\mathbf{Q}) - \mathbf{L}(\mathbf{k}, 0, -\mathbf{Q}) Y^2(\mathbf{k}, +\mathbf{q}, -\mathbf{Q})], \quad (14c)$$

$$J_3 = \frac{e\hbar}{2mV} \sum_{q/2 > k_z > 0} \Delta^*(k_n) K_{k, k-q-Q}^{-Q} [\mathbf{L}(\mathbf{k}, -\mathbf{q}, -\mathbf{Q}) Y^2(\mathbf{k}, 0, -\mathbf{Q}) - \mathbf{L}(\mathbf{k}, 0, -\mathbf{Q}) X^2(\mathbf{k}, 0, -\mathbf{Q})], \quad (14d)$$

$$J_4 = \frac{e\hbar}{2mV} \sum_{-q/2 < k_z < 0} \Delta(k_x) K_{k, k+q-Q}^{-Q} [\mathbf{L}(\mathbf{k}, +\mathbf{q}, -\mathbf{Q}) Y^2(\mathbf{k}, 0, -\mathbf{Q}) - \mathbf{L}(\mathbf{k}, 0, -\mathbf{Q}) X^2(\mathbf{k}, 0, -\mathbf{Q})]. \quad (14e)$$

Assuming symmetry in the  $\pm k_y$  direction in the reciprocal lattice, and substituting free-electron values  $E_k = \hbar^2 k^2 / 2m$ , etc., we find for  $J_1$  a current only in the  $x$  direction, given by

$$J_1 = \left[ \frac{e\hbar}{2mV} \right] \sum_{k_z > q/2} \Delta^*(k_x) \Lambda(k_x) k_x X^2(\mathbf{k}, -\mathbf{q}, -\mathbf{Q}) (2m / \hbar^2 Q) (2m / \hbar^2) [q k_z (q - k_z)]^{-1}. \quad (15)$$

From Eq. (13b),

$$X^2(\mathbf{k}, -\mathbf{q}, -\mathbf{Q}) \simeq Q \frac{\partial}{\partial K_z} |x_{\mathbf{k}}|^2_{\mathbf{K}=\mathbf{k}-\mathbf{q}}. \quad (16)$$

Using the nearly-free-electron approximation, we find, in terms of  $\tilde{E}_k$ , the eigenvalues, that

$$\begin{aligned} \frac{\partial}{\partial K_z} |x_{\mathbf{k}}|^2 &= -2 |x_{\mathbf{k}}|^2 |y_{\mathbf{k}}|^2 \\ &\times [\partial(\tilde{E}_K - E_K) / \partial Q] / (\tilde{E}_K - E_K) \\ &\approx \frac{\hbar^2}{2m} |x_{\mathbf{k}}|^2 |y_{\mathbf{k}}|^2 q / \Lambda; \end{aligned} \quad (17)$$

the latter approximation holds in the vicinity of the gap, i.e., where  $\tilde{E}_K - E_K \sim \Lambda$ .

We recall that  $\Lambda(k_x)$  is to be found by a variational calculation. Comparing Eq. (7) for  $H_{qs}$  with the form of  $H_A$ , we make the convenient replacement

$$\Lambda(k_x) = s A(k_x / |k_x|)(q/2) \frac{e\hbar}{(2m)}. \quad (18)$$

$s$  will be the parameter of variation. It is dimensionless.  $\Lambda(k_x)$  is taken here as odd in  $k_x$ . Actually, we shall single out the odd components in  $\Delta(k_x) \Lambda(k_x)$ , taking the product of one even and one odd component, and the reverse. At the same time Eq. (18) shows explicitly that  $H_{qs}$  is to be thought of (it will be) as linear in the applied

vector potential  $A$ ,  $A \equiv |\mathbf{A}(Q)|$ . Combining the last four equations and similarly reducing  $J_2$  we find

$$J_1 + J_2 \sim s A (\hbar e / m)^2 (1 / \epsilon_B) (1 / V) \sum k_x q |x_{\mathbf{k}}|^2 |y_{\mathbf{k}}|^2, \quad (19)$$

again in the vicinity of the gap. The sum in Eq. (19) is roughly restricted to values of  $k_z$ :

$$\frac{q}{2} \left[ 1 + \frac{2\Delta}{\epsilon_B} \right] > k_z > \frac{q}{2} \left[ 1 - \frac{2\Delta}{\epsilon_B} \right].$$

One also finds that  $J_3 + J_4 = J_1 + J_2$ , so that, finally,  $J$  is in the  $x$  direction and

$$J \sim s J_A (\Delta / \epsilon_B), \quad (20a)$$

where  $\Delta / \epsilon_B$  is the ratio of half the gap to the band width, i.e.,

$$\epsilon_B = \hbar^2 q^2 / 8m \quad (20b)$$

and

$$J_A = e^2 n A / mV. \quad (20c)$$

The logarithmic singularity resulting from the pole at the center of the Brillouin zone in Eq. (15) is removed when we work to higher order in  $Q$ . It is expected to disappear altogether if a model involving a more symmetric mixture than just two waves,  $\mathbf{k}, \mathbf{k}+\mathbf{q}$  for  $k_z < 0$

and  $\mathbf{k}, \mathbf{k}-\mathbf{q}$  for  $k_z > 0$ , is used. Actually, as we go from the gap at  $k_z = \pm q/2$  towards the center of the zone,  $X^2(\mathbf{k}, -\mathbf{q}, -\mathbf{Q})$  diminishes rapidly. The source of the supercurrent, not surprisingly, is near the edge of the Brillouin zone. Here the usual nearly-free-electron model we are using is appropriate.

### VARIATIONAL CALCULATION

Turning to Eq. (6) we have that  $\langle H_{AA} + \frac{1}{2}[H_A, K_I] \rangle$  gives the usual diamagnetism of an insulator. Some matrix manipulation along with Eq. (5) easily shows that for the crossterms in Eq. (6) one gets

$$\langle \frac{1}{2}[H_A, K_s] + \frac{1}{2}[H_{qs}, K_I] \rangle = - \int \mathbf{A}(\mathbf{r}) \cdot \mathbf{J}_s(\mathbf{r}) dv. \quad (21)$$

Last, again from Eq. (5), one finds that  $\frac{1}{2}\langle [H_{qs}, K_s] \rangle$  is the second-order perturbation term

$$- \sum_n | \langle 0 | H_{qs} | n \rangle |^2 / (E_n - E_0).$$

It represents the interaction of the conduction band and the modes  $\pm q - Q$  in the absence of any vector potential  $\mathbf{A}$ . This term is part of the energy of lattice deformation in these modes, which we now balance against the electromagnetic term in Eq. (21), yielding the desired value of  $s$ .

To find the energy stored in the lattice  $U \sim 4\hbar\omega_{q+Q}n_{q+Q}$ , with  $n_{q+Q}$  the number of phonons in the mode, we first note that in view of Eq. (8),  $\Lambda \approx g(n_{q+Q}/V)^{1/2}$ , with  $g$  the usual electron-phonon coupling constant and  $V$  the volume of the sample. We wish to minimize with respect to  $s$  the energy

$$U - \int \mathbf{A}(\mathbf{r}) \cdot \mathbf{J}_s(\mathbf{r}) d^3r \\ = 4s^2\hbar\omega_{q+Q}\epsilon_B e^2 A^2 (g^2 V^{-1} m)^{-1} - s A J_A (\Delta/\epsilon_B) V, \quad (22)$$

where we have used Eq. (9). We find

$$s \approx \frac{1}{8} (n/V) g^2 (\hbar\omega_{q+Q} \epsilon_B)^{-1} (\Delta/\epsilon_B). \quad (23)$$

If we take  $n \approx 10^{22}$  electrons/cm<sup>3</sup>,  $g^2 \approx 10^{-31}$  eV<sup>2</sup> cms<sup>3</sup>, and  $\epsilon_B \approx 4$  eV, then we find that for  $s \approx \Delta/\epsilon_B$  we need a mode softening to about  $\omega_{q+Q} \approx 10^4$  rad/s. This gives a supercurrent  $\sim J_A (\Delta/\epsilon_B)^2$ . From the lattice stability of the phase until at least 180 K,<sup>3</sup> we infer that  $\Delta$  is at least  $kT$  with  $T \sim 200$  K. A similar gap, i.e., 25–50 MeV, was deduced from quite independent experiments in applied electric fields by Doding and Labusch.<sup>25</sup> Thus, we have current densities of the same order of magnitude as are found in superconducting metals, where  $J \approx J_A (kT_c/E_F)$ . Given the extreme observed instability of the material, softness with  $\omega_{q+Q} \approx 10^4$  rad/s may be well forthcoming. For electron-phonon coupling we have used typical deformation potential constants. Less conservatively, if piezoelectric coupling values are used, even larger values of current will be obtained; alternatively less softening will suffice.

We have so far ignored temperature. Our aim has been

to discover some possible mechanism to fit in with the observations. In this endeavor we regard temperature as a second-order effect. We again note that we are dealing with a gap of at least 25 MeV, very large in the context of metallic superconductivity.

### DISCUSSION

We are left with several questions. One is how does the Cl doping have such a strong influence on the lattice structure? It is to be supposed that the Cl ions go in substitutionally, and become donors. From the careful chemical analysis provided us by the Koch and Stoltz,<sup>9</sup> we are able to verify that these are compensated by  $S$  vacancies, leading to  $F$ -center acceptors. We suppose further that strain associated with the modes that take us from zinc-blende structure to wurzite raises the energy of these centers. In fact, conductivity measurements show that the activation energy associated with conductivity increases from about 0.35 to 0.7 eV as we go through the phase change at  $C^*$ . Therefore, the energy of formation of centers also changes, and the free-energy change must be presumed sufficient to drive the phase change.

Of interest also is the cubic-to-wurzite change after pressure quenching. In this case the resulting wurzite is observed to have a much lower resistivity. We presume that here the phase change induces an overlap between the top of a valence subband and the  $F$ -center energy levels, causing some electrons to be transferred out of the subband as the phase change proceeds. Labbé and Friedel suggested a somewhat similar mechanism of electron transfer between  $d$  bands to account for martensitic phase changes occurring in  $A15$  compounds,<sup>26</sup> and Kragler and Thomas made such an electron transfer an integral part of the mechanism for explaining the softening of shear modes in these compounds.<sup>27</sup>

Also of concern is the observation that immediately upon pressure quenching the material tends to be diamagnetic with, however, the paramagnetic phase always emerging as the stable situation after some days. The development here has been for the simplest situation possible. In fact, many other forces may be driving the lattice deformation than the flow of current in the applied magnetic field. There comes to mind the new high- $T_c$  ceramic superconductors that are just witnessing a most rapid development.<sup>28</sup> Here there is direct coupling between applied magnetic fields and ionic spins. It seems plausible that exchange forces or direct electrostatic fields then result in lattice deformations. The gist of our development is that induced lattice deformations lead to supercurrents. Returning to the initial unstable phase of CdS, the heterogeneous and soft state of the specimens upon quenching is apt to be complicated, possessing a domain structure. We can speculate that the structural deformations induced by the magnetic field would be in the direction of a stable lattice. They would not necessarily correspond to the energy states sought out by our idealized variational calculation.

Last, we point out that alternative explanations of the data are a possibility. We have been informed that recent

experiments by the Zürich group with  $\text{La}_{2-x}\text{Ba}_x\text{CuO}_4$  point to electron pairing. The situation may or may not be the same in CdS. In any case we note that our treatment, a perturbation calculation for small vector potential  $A$ , only allows the phenomena to be understood inasmuch as they are a continuous function of  $A$ . We plan as a next step to study the implications of our model as regards flux quantization before considering possible modifications.

#### ACKNOWLEDGMENTS

We acknowledge support by the U.S. Air Force Office of Scientific Research under Contract No. AF0SR-79-0216, U.S. Army Research under ARRADCOM Contract No. ARRADCOM No. 5004-07-001 and the U.S. Office of Naval Research under Contract No. N00014-80-C-0929, and Department of Energy DOE Grant No. DE-F902-84ER 45098.

\*Present address: Perkin-Elmer Corporation, Norwalk, CT 06854.

†Present address: Jet Propulsion Laboratory, Pasadena, CA 91109.

<sup>1</sup>E. Brown, C. G. Homan, and R. K. MacCrone, *Phys., Rev. Lett.* **45**, 478 (1980).

<sup>2</sup>C. G. Homan and R. K. MacCrone, *J. Non-Cryst. Solids* **40**, 369 (1980).

<sup>3</sup>C. G. Homan and R. K. MacCrone, *Ferroelectrics* **73**, 481 (1987); in *High Pressure in Science and Technology, Part I*, Proceedings, of the 9th Association International des Recherches pour l'Avancement de Technologie à haut Pressure International Conference, Albany, N.Y., 1983, edited by C. G. Homan, R. K. MacCrone, and E. Whalley (North-Holland, New York, 1986), Vol. 22, p. 187.

<sup>4</sup>A preliminary report of the theory will be published in *Z. Phys. B* **68**, 139 (1987).

<sup>5</sup>R. Sato, *Acta Crystallogr.* **15**, 1109 (1962).

<sup>6</sup>R. Sato, H. Itoh, and S. Yamashita, *Jpn. J. Appl. Phys.* **3**, 626 (1964).

<sup>7</sup>R. O. Miller, F. Dache, and R. Roy, *J. Appl. Phys.* **37**, 4913 (1966).

<sup>8</sup>P. J. Cote, C. G. Homan, W. C. Moffat, S. Block, G. P. Piermarini, and R. K. MacCrone, *Phys. Rev. B* **28**, 5041 (1983).

<sup>9</sup>W. F. Koch and J. W. Stoltz, *Anal. Chem.* **54**, 340 (1982).

<sup>10</sup>M. A. Short and E. G. Steward, *Am. Mineral.* **44**, 189 (1959).

<sup>11</sup>D. P. Koistinen and R. E. Marburger, *Trans. Am. Soc. Met.* **51**, 537 (1959).

<sup>12</sup>B. E. Warren, *X-Ray Diffraction* (Addison-Wesley, Reading, MA, 1969), p. 298.

<sup>13</sup>A. Rosenzweig, *Photoacoustics and Photoacoustic Spectroscopy* (Wiley, New York, 1979).

<sup>14</sup>R. Florian, J. Pelzl, M. Rosenberg, and H. Vargas, *Phys. Status Solidi A* **48**, K35 (1978).

<sup>15</sup>J. Pelzl, P. Engels, and R. Florian, *Phys. Status Solidi B* **82**,

145 (1977).

<sup>16</sup>J. Pelzl, K. H. Hock, A. J. Miller, P. J. Ford, and G. A. Saunders, *Z. Phys. B* **40**, 321 (1981).

<sup>17</sup>P. Korpium, R. Tilgner, and D. Schmidt, in Proceedings of the Third International Topical Meeting on Photoacoustic and Photothermal Spectroscopy, Paris, 1983 edited by J. Badoz and D. Fournier [*J. Phys. (Paris) Colloids* **44**, C6-43 (1983)].

<sup>18</sup>K. Junge, B. Bein, and J. Pelzl, in Proceedings of the Third International Topical Meeting on Photoacoustic and Photothermal Spectroscopy, Paris, 1983, Ref. 17.

<sup>19</sup>G. Wentzel, *Phys. Rev.* **111**, 1488 (1958).

<sup>20</sup>H. Frohlich, *Proc. R. Soc. London, Ser. A* **223**, 296 (1954).

<sup>21</sup>D. Allender, J. W. Bray, and J. Batdeen, *Phys. Rev. B* **9**, 119 (1974).

<sup>22</sup>G. Wentzel, *Phys. Rev.* **83**, 168 (1951).

<sup>23</sup>W. Kohn and Vachaspati, *Phys. Rev.* **83**, 462 (1951).

<sup>24</sup>We find that  $\Lambda$  is real. A formal way of handling the phonon field, with creation and destruction operators  $b_{q-Q}^*, b_{q-Q}$ , is given by intermediate-coupling theory [T. D. Lee and D. Pines, *Phys. Rev.* **88**, 960 (1952)]. Following others we have here developed more physically, avoiding additional formalism. Our  $\Lambda, \Lambda^*$ , which in intermediate coupling would have also been variationally by the same equations, are proportional, respectively, to  $\langle b_{q-Q}^* \rangle, \langle b_{q-Q} \rangle$ .  $\Lambda$  real means a shift in displacement, but not in momentum. We have lattice deformations in space synchronization with the static applied field  $\mathbf{A}(\mathbf{r})$ .

<sup>25</sup>G. Doding and R. Labusch, *Phys. Status Solidi A* **68**, 409 (1981).

<sup>26</sup>J. Labbé and J. Friedel, *J. Phys. (Paris)* **27**, 153 (1966).

<sup>27</sup>R. Kragler and H. Thomas, *J. Phys. (Paris) Lett.* **36**, L153 (1975).

<sup>28</sup>J. G. Bednorz and K. A. Muller, *Z. Phys. B* **64**, 189 (1986).